



**Alternating Phase Shift Mask (PSM) Phase Defect Printability
for 130 nm and 100 nm KrF Lithography**

SEMATECH and the **SEMATECH logo** are registered service marks of SEMATECH, Inc.
International SEMATECH and the **International SEMATECH logo** are registered service marks
of International SEMATECH, Inc., a wholly-owned subsidiary of SEMATECH, Inc.

Product names and company names used in this publication are for identification purposes only
and may be trademarks or service marks of their respective companies.

Alternating Phase Shift Mask (PSM) Phase Defect Printability for 130 nm and 100 nm KrF Lithography

Technology Transfer # 00033918A-TR

International SEMATECH

May 19, 2000

Abstract: This document covers a study to determine the maximum non-printable phase defects for 130 nm and 100 nm linewidths by using a KrF deep ultraviolet (DUV) scanner. It is part of an effort to extend optical lithography to the sub-wavelength region for very low K1 patterning processes. This study used resist simulations verified by wafer printing results to predict printable defects for denser patterns. It also tested mechanical repair tools for phase bump defects and compared electromagnetic field (EMF) three-dimensional simulation with commercialized two-dimensional tools for phase defect printability.

Keywords: Atomic Force Microscopy, Critical Dimension, Deep Ultraviolet Lithography, Phase Shifting Masks, Defect Detection, Pattern Defects, Scanning Electron Microscopy

Authors: Juhwan Kim, Wang-Pen Mo, Ron Gordon, Alvina Williams

Approvals: Young-Sik Kim, Project Manager
Dan McGowan, Technical Information Transfer Team Leader

Table of Contents

1	EXECUTIVE SUMMARY.....	1
2	INTRODUCTION.....	1
3	EXPERIMENTAL PROCEDURES	2
3.1	Overall Experimental Process Flow	2
3.2	Programmed Defect Mask Design.....	2
3.3	Mask Pattern Metrology	2
3.4	Wafer Printing Process Condition	3
3.5	Definition of Printable Defects	3
4	RESULTS AND DISCUSSION	3
4.1	Programmed Defect Mask Fabrication	3
4.2	Wafer Printing Results on Defect Printability	4
4.2.1	L/S=140 nm/360 nm Pattern	4
4.2.2	L/S=100 nm/400 nm Pattern	7
4.3	Aerial Image Simulation vs. Resist Process Simulation for Defect Printability.....	9
4.4	3D EMF vs. 2D Aerial Image Simulation for Phase Defect Printability.....	11
4.5	Defect Printability Prediction for Denser Pattern of L/S=130 nm/130 nm	13
4.6	Phase Bump Defect Repair	14
5	CONCLUSION AND FUTURE WORKS	16
6	REFERENCES.....	17

List of Figures

Figure 1	Chrome Defects and 180° Phase Bumps.....	2
Figure 2	Defect Size Measurement	3
Figure 3	CD SEM Defect Size Measurement Results (Programmed Size vs. Measured Size)	4
Figure 4	Edge Phase Bump Defect Pattern; Chrome Etched Away from Line Edge	4
Figure 5	Defect Size vs. Linewidth of L/S = 140 nm/360 nm Pattern with Focus Variation.....	5
Figure 6	Expose/Defocus Window of L/S = 140 nm/360 nm Pattern.....	6
Figure 7	MNPD Comparison Between Defocus Only and Expose/Defocus Window of L/S = 140 nm/360 nm Pattern.....	7
Figure 8	Defect Size vs. Linewidth of L/S – 100 nm/400 nm Pattern with Focus Variation.....	7
Figure 9	Expose/Defocus Window of L/S = 100 nm/400 nm Pattern.....	8
Figure 10	MNPD Comparison Between Focus Only and Expose/Defocus Window of L/S = 100 nm/400 nm Pattern.....	8
Figure 11	Defect Size vs. Linewidth Comparison Between Aerial Image and Resist Simulation of L/S = 140 nm/360 nm Pattern	9
Figure 12	Defect Size vs. Linewidth Comparison Between Aerial Image and Resist Simulation of L/S = 100 nm/400 nm Pattern	10
Figure 13	Simulated Result Comparison Between Defocus Only and Expose/Defocus Window.....	10
Figure 14	Aerial Image Comparison Between 2D Simulation and 3D EMF Simulation of L/S = 140 nm/360 nm Pattern with 390 nm Phase Defect	11
Figure 15	Defect Size vs. Linewidth Simulation Plot Comparison Between 2D Aerial Image Simulation and 3D EMF Simulation of L/S = 130 nm/370 nm Pattern.....	12
Figure 16	Defect Size vs. Linewidth Simulation Plot Comparison Between 2D Aerial Image Simulation and 3D EMF Simulation of 1:4 Duty Ratio Pattern and 1:2 Duty Ratio Pattern.....	12
Figure 17	Defect Size vs. Linewidth Simulation Plot comparison Between 2D Aerial Image Simulation (Shadow) and 3D EMF Simulation of L/S = 30 nm/370 nm Pattern	13
Figure 18	Defect Size vs. Linewidth Simulation Plot Comparison Between Aerial Image and Resist Simulation of L/S = 130 nm/130 nm.....	14
Figure 19	Phase Bump Defect Pattern Images Before and After Repair by Mechanical Removal Tool.....	15
Figure 20	Expose/Defocus Windows of Phase Bump Center Defect Pattern of L/S = 140 nm/360 nm Before and After Repair by Mechanical Removal Tool.....	16
Figure 21	Expose/Defocus Windows of Phase Bump Edge Defect Pattern of L/S = 140 nm/360 nm Before and After Repair by Mechanical Removal Tool.....	16

List of Tables

Table 1	MNPD Size Comparison Between Traditionally Defined Case and Window Overlap Cases	9
Table 2	MNPD Size Comparison Between Aerial Image Simulation and Resist Simulation	10
Table 3	MNPD Size Comparison Between Traditionally Defined Case and Window Overlap Cases by Resist Simulation	11
Table 4	MNPD Size Comparison Between 2D Aerial Image and 3D EMF Simulation	13
Table 5	Simulated MNPD Size for 1:1 Dense Pattern of L/S=130 nm/130 nm	14

Acknowledgements

The authors wish to acknowledge Wally Carpenter and Wayne Smith at International SEMATECH for their support this work. We also thank Barry Hopkins at RAVE for repair work, and Asmita Shah for AFM images collection.

1 EXECUTIVE SUMMARY

Optical lithography is pushed more to extend to sub-wavelength region for very low K1 patterning processes. In this, alternating phase shift mask (PSM) is the solution for isolated patterns, without changing the wavelength of exposure tools' light source. With this prospect, critical issues such as design layout complexity, light intensity imbalance between shifted and unshifted space area, and phase defect controllability recently have been studied in order to apply alternating PSM for mass production of devices.

This report recounts a study to find out the maximum non-printable phase defects for 130 nm and 100 nm lines by printing the wafer using a KrF deep ultraviolet (DUV) scanner. With the limitations of the mask making process for very small programmed defects, masks with duty ratio around 1:3 have been made. After resist simulation for the test pattern was verified by wafer printing results, printable defects for denser pattern were predicted.

In addition to the defect printability study, mechanical repair tools for phase bump defects were tested using 248 nm AIMS, atomic force microscopy (AFM), and critical dimension scanning electron microscopy (CD SEM) metrology, as well as wafer printing. Electromagnetic field (EMF) three-dimensional (3D) simulation also was compared with a commercialized two-dimensional (2D) simulation tool for phase defect printability.

2 INTRODUCTION

Optical lithography is pushed more to extend to sub-wavelength region for very low K1 patterning processes, in which alternating PSM is the solution for isolated patterns without changing the wavelength of exposure tools' light source. With this prospect, the critical issues such as design layout complexity, light intensity imbalance between shifted and unshifted space area [1,2], and phase defect controllability [3,4] recently have been studied in order to apply alternating PSM for device mass production.

Especially, discriminating the non-printable defects from the printable defects is becoming more important to mask manufacturers, not only for mask making process itself, but also for determining the specifications of inspection tools and repair tools within reasonable tool development cost.

However, while all the literatures have considered the exposure tool's defocus for defect printability study, few of them have included exposure dose as a factor for it. In addition, they have used aerial image simulation to predict the printable defects, but resist process factors cannot be neglected, especially for low K1 process.

This project studied phase defect printability for 130 nm and 100 nm lines of 500 nm pitch by printing the wafer using programmed defect masks and a KrF DUV scanner. Using experimental results, printability was compared by considering only the scanner's focus factor, and by looking at both exposure dose and focus factors.

Aerial image simulation and resist process simulation were compared to actual wafer printing results, verifying the defect printability prediction for 130 nm and 100 nm lines of 500 nm pitched pattern using a two-dimensional (2D) simulation tool.

Two-dimensional simulation was compared to 3D electromagnetic field simulation for the printability of phase bump defects and divot defects. Based on verified defect simulation for ~1:3 duty ratio test patterns, printable phase defects for denser pattern were predicted.

Mechanical repair tool was tested for printable quartz bumps using 248 nm AIMS, AFM, and CD SEM metrology, as well as wafer printing.

3 EXPERIMENTAL PROCEDURES

3.1 Overall Experimental Process Flow

After the programmed defect mask was fabricated, experimenters measured the mask pattern CDs and actual defect sizes using CD SEM. Based on this mask pattern information, wafer printing was done and analyzed to define printable defects. Duty ratio patterns of 1:3 were verified from experimental data, aerial image simulation, and resist process simulation.

Afterward, printable phase defects for denser pattern were predicted using a verified simulation approach. Regarding phase defects repair tool evaluation, several printable quartz defects were removed and inspected using CD SEM, AFM, 248 nm AIMS, and wafer printing test, before and after repair.

3.2 Programmed Defect Mask Design

With the limitations of the mask making process for very small programmed phase defects, the masks were made with duty ratio around 1:3. Wet etch processing after dry etch was omitted to get very small phase defects. Lines and space patterns at 130 nm/370 nm and 100 nm/400 nm were applied for wafer printing test. Three different phases, 60/120/180°, were made for phase bump defects and divot defects, as well as chrome defects. All programmed defects were located at the center and edge of the patterns, as shown in Figure 1. The experiment was limited to chrome defects and 180° phase bump defects.

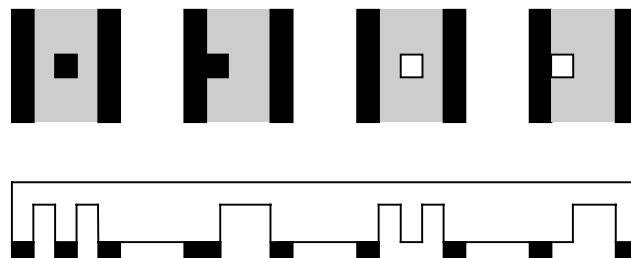


Figure 1 Chrome Defects and 180° Phase Bumps

3.3 Mask Pattern Metrology

A KLA8100R CD SEM was used to measure pattern CDs and defects sizes on the mask. The defect sizes on the mask were measured by diameter of the inside circles, as shown in Figure 2. To evaluate the mechanical repair tool's capability of quartz bump defect removal, AFM, CD SEM and 248 nm AIMS images were captured both before and after repair. Those images were compared to wafer printing results.

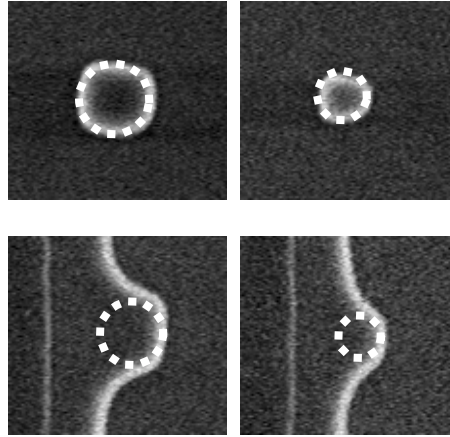


Figure 2 Defect Size Measurement

3.4 Wafer Printing Process Condition

An SVGL MS3 KrF DUV scanner and UV6 resist were used for printing the wafer. Illumination conditions were 0.6 na and 0.3σ . The resist thickness was 540 nm and coated on DUV 30 organic bottom antireflective coating (ARC). Exposure dose and focus matrices were shot on the wafer so that the process window of defective pattern linewidths could be compared to non-defective pattern linewidth.

3.5 Definition of Printable Defects

Traditionally, the standard wafer CD is defined as that printed line width included in the region surrounded by the lines corresponding to specified focus range and wafer CD target $\pm 10\%$ on through focus plots. A $0.4 \mu\text{m}$ focus range was used for this study, based on the process window of no defect patterns.

However, experimenters calculated the process window overlap between defect patterns and no defect patterns for various defect sizes in order to include the expose dose process factor to printability study. This process window overlap approach was compared with traditional methods to investigate the relationship between them. The term “maximum non-printable defect” (MNPD) was used because it is more useful to mask users rather than is minimum printable defect. Also, this study measured wafer CD of the linewidth next to programmed defects.

4 RESULTS AND DISCUSSION

4.1 Programmed Defect Mask Fabrication

In case of phase bump defects, programmed defects were generated as small as 60 nm at center and 40 nm at the edge of the pattern on the mask. Also, 180° phase bump defects were generated at almost the same sizes as chrome defects, as shown in Figure 3. Experimenters could not get phase divot defects smaller than 700 nm on the mask because of the second writer’s resolution limit.

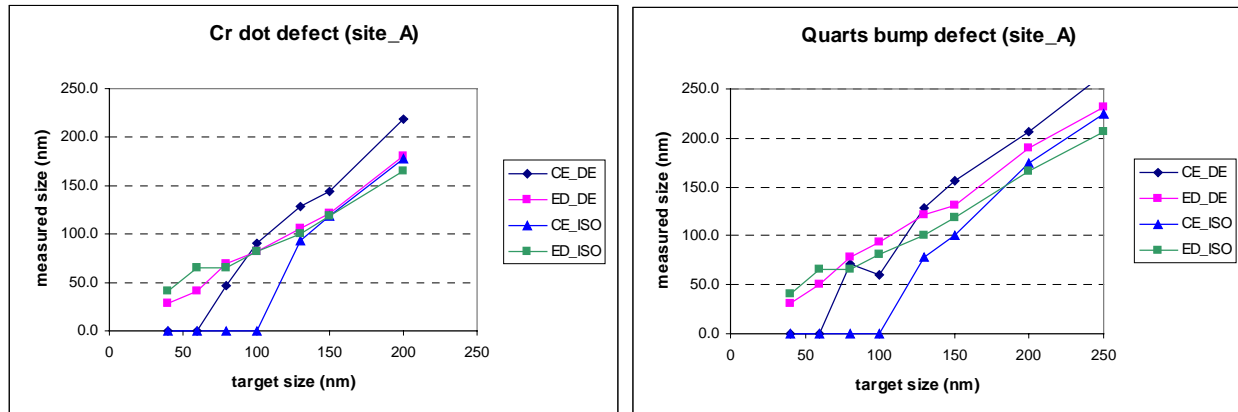


Figure 3 CD SEM Defect Size Measurement Results (Programmed Size vs. Measured Size)

It also was discovered that chrome layer was unexpectedly removed at the pattern where the phase bump edge defects are located, due to the limited registration ability of the second writer. This chrome removed pattern caused pattern position shift compared to non-attacked pattern, as shown in Figure 4.

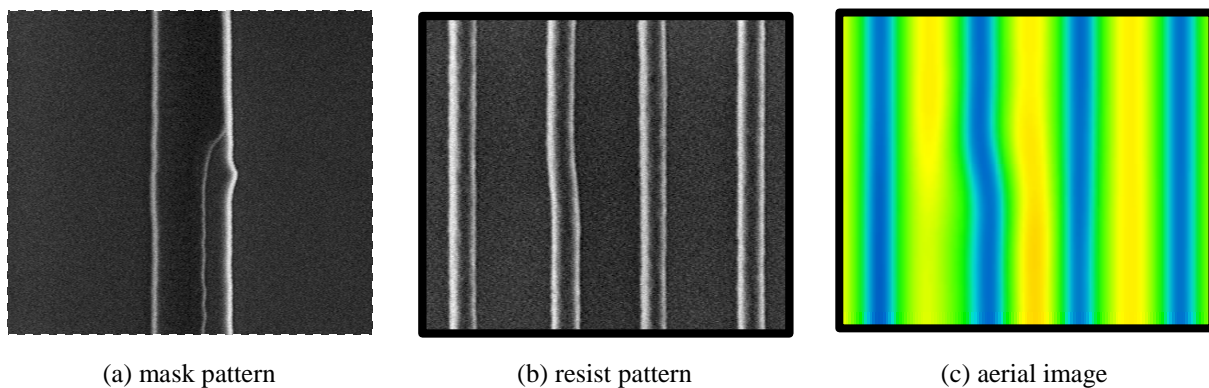


Figure 4 Edge Phase Bump Defect Pattern; Chrome Etched Away from Line Edge

4.2 Wafer Printing Results on Defect Printability

4.2.1 L/S=140 nm/360 nm Pattern

The target pattern size was changed from L/S=130 nm/370 nm to L/S=140 nm/360 nm, based on mask CD measurement. With the traditional definition of printability, which considers only focus range at optimum expose dose, MNPD sizes were 320 nm for chrome center defect, 305 nm for 180° phase bump center defect, 270 nm for chrome edge defect, and 280 nm for phase bump edge defect, as shown in Figure 5.

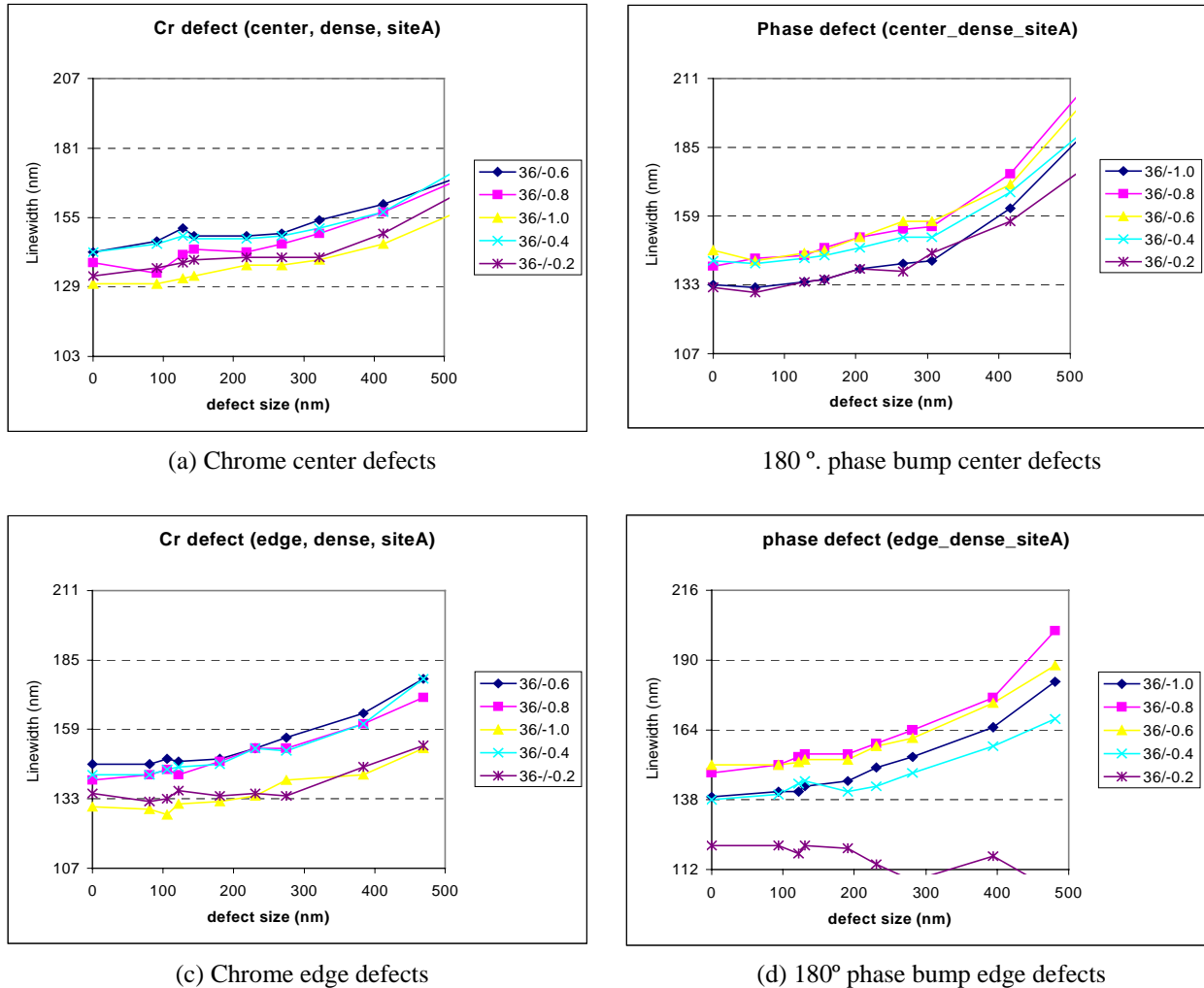
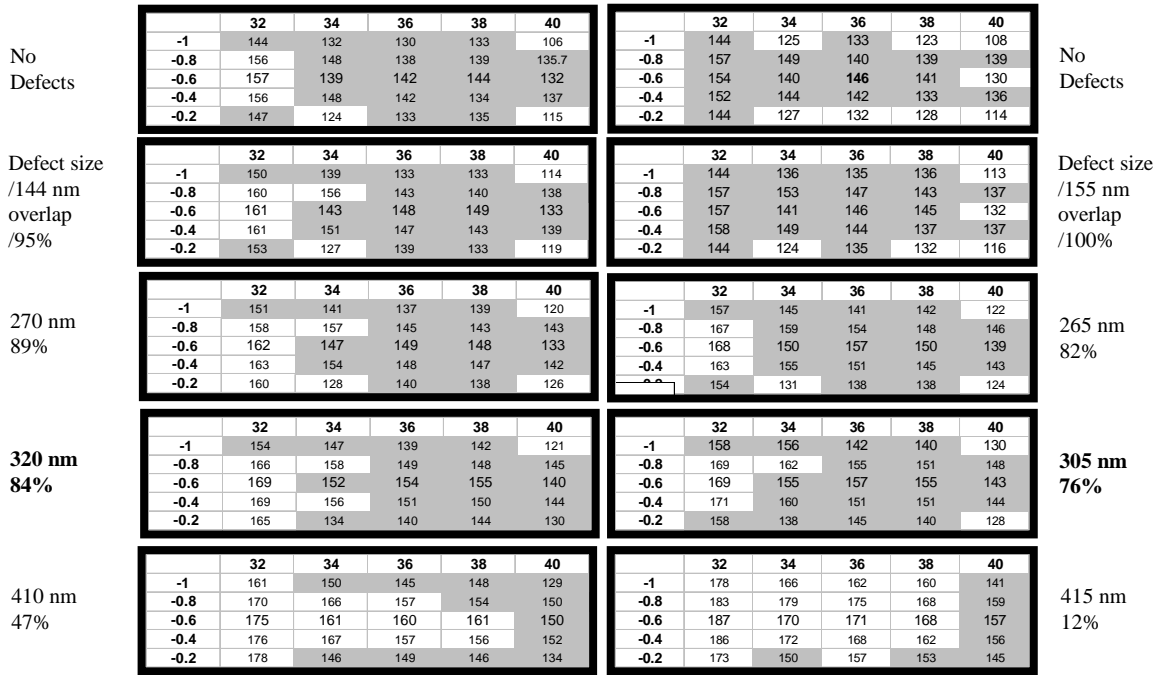


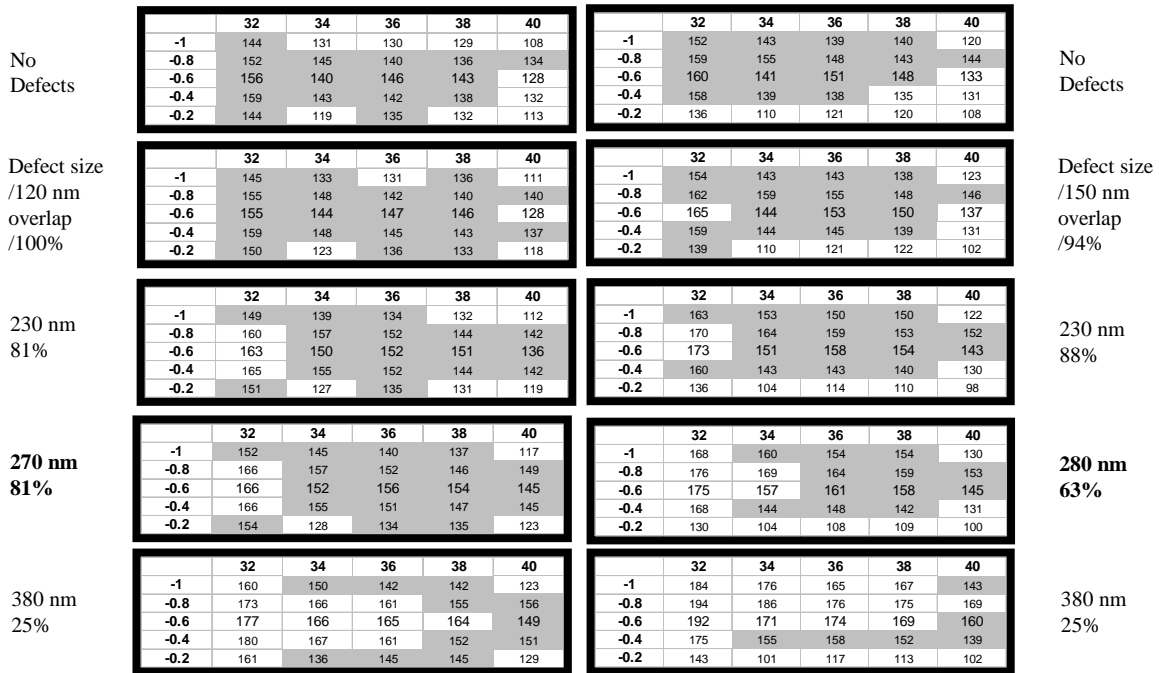
Figure 5 Defect Size vs. Linewidth of L/S = 140 nm/360 nm Pattern with Focus Variation

When the process window overlap method was applied between defect pattern and no defect pattern, traditionally defined MNPD sizes showed 84% overlap for chrome center defect, 76% overlap for phase bump center defect, 81% chrome edge defect, and 63% overlap for phase bump edge defect, as shown in Figure 6.



(a) Chrome center defects

(b) 180° phase bump center defects



(c) Chrome edge defects

(d) 180° phase bump edge defects

Figure 6 Expose/Defocus Window of L/S = 140 nm/360 nm Pattern

For 140 nm/360 nm lines and spaces pattern, chrome defects and phase bump defects smaller than 230 nm keep the process window overlap at least 80% as shown in Figure 7.

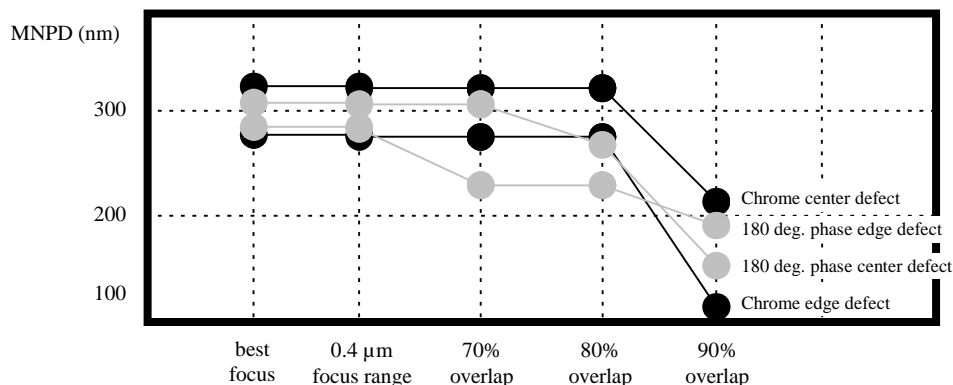


Figure 7 MNPDP Comparison Between Defocus Only and Expose/Defocus Window of L/S = 140 nm/360 nm Pattern

4.2.2 L/S=100 nm/400 nm Pattern

For L/S=100 nm/400 nm pattern, MNPDP sizes of traditional method were 150 nm for phase bump center and edge defect, as shown in Figure 8.

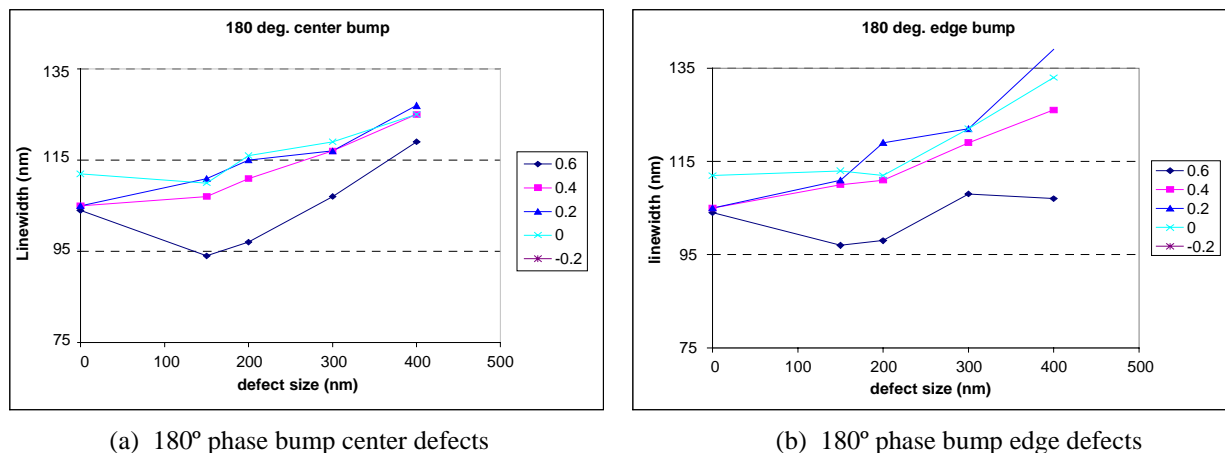


Figure 8 Defect Size vs. Linewidth of L/S – 100 nm/400 nm Pattern with Focus Variation

When the process window overlap method was applied, 150 nm phase bump defects showed 72% overlap for center defect and 83% overlap for edge defect, as shown in Figure 9.

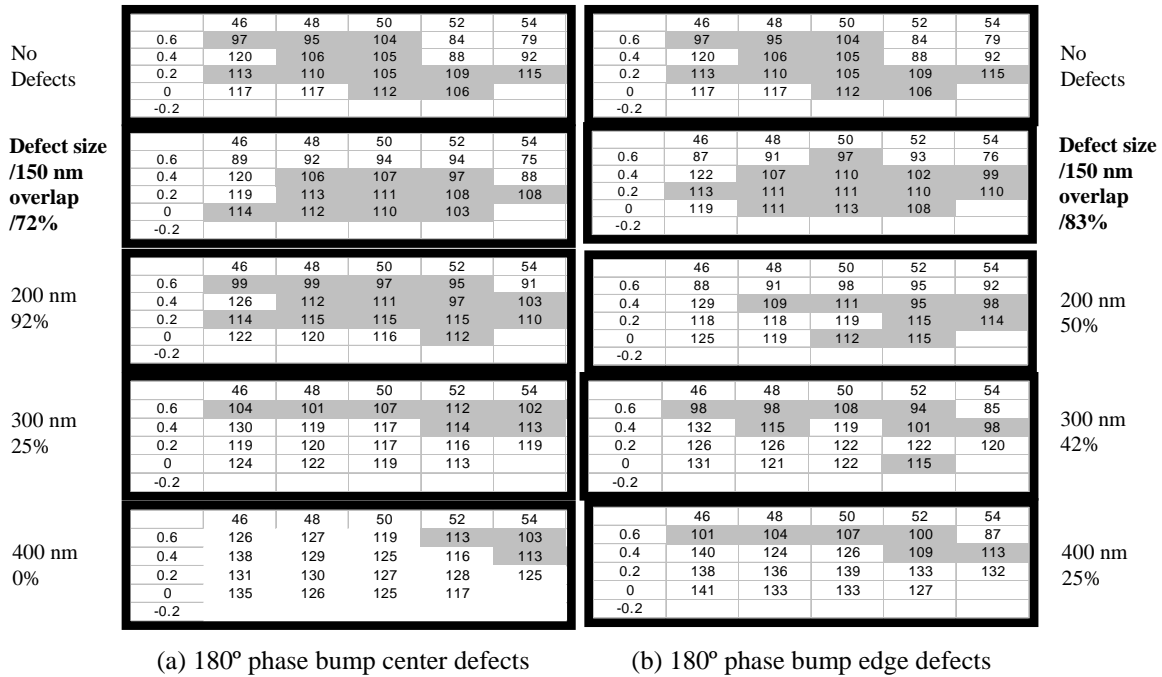


Figure 9 Expose/Defocus Window of L/S = 100 nm/400 nm Pattern

It was found that traditionally defined MNPD sizes for 100 nm/400 nm pattern also showed around 80% overlap for phase bump defects, as shown in Figure 10.

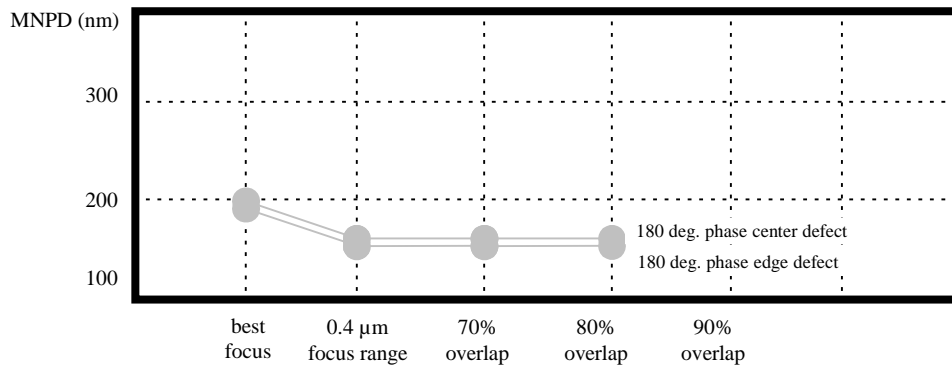


Figure 10 MNPD Comparison Between Focus Only and Expose/Defocus Window of L/S = 100 nm/400 nm Pattern

Based on the Table 1, 70% to 80% process window overlap can be expected between defect pattern and no defect pattern if an MNPD-sized defect exists at pattern of L/S=140 nm/360 nm and 100 nm/400 nm.

Table 1 MNPD Size Comparison Between Traditionally Defined Case and Window Overlap Cases

	L/S=140 nm/360 nm				L/S=100 nm/400 nm	
	Chrome		Phase bump		Phase bump	
	Center	Edge	Center	Edge	Center	Edge
Traditional way	320	270	305	280	150	150
70% overlap	320	270	305	230	150	150
80% overlap	320	270	265	230	—	150
90% overlap	144	120	155	190	—	—

4.3 Aerial Image Simulation vs. Resist Process Simulation for Defect Printability

Aerial image simulation and resist simulation were done for the same patterns of L/S=140 nm/360 nm and 100 nm/400 nm, and compared to experimental results. Experimenters used the UV6 resist parameters of baseline lithography process at International SEMATECH. The square-shaped defects were applied for the defect pattern simulation.

As a result, aerial image simulation data were very to the experimental data, while resist simulation tended to overestimate defect printability compared to experimental data, as shown in Figure 11, Figure 12, and Table 2.

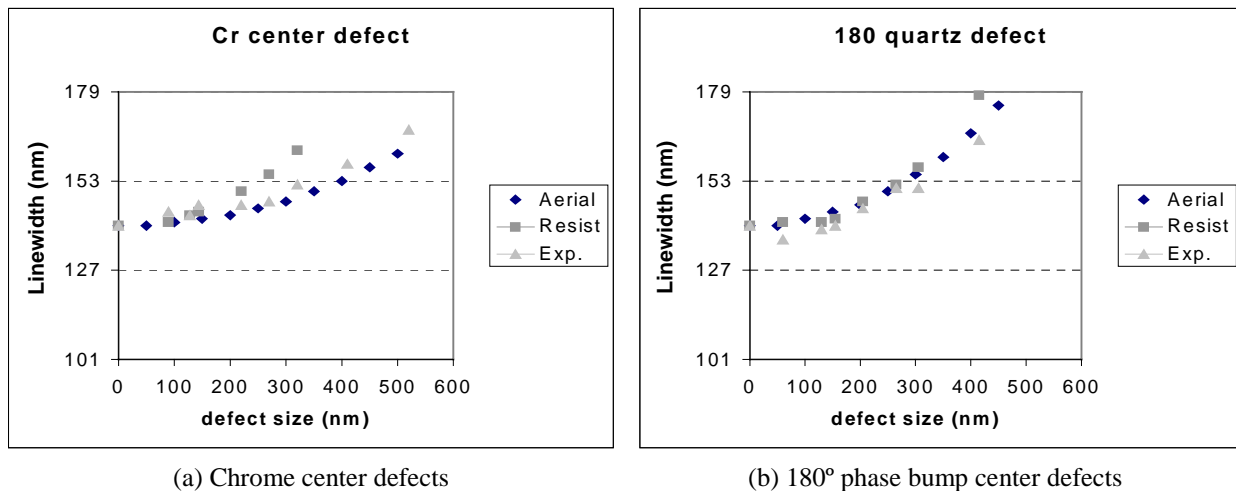


Figure 11 Defect Size vs. Linewidth Comparison Between Aerial Image and Resist Simulation of L/S = 140 nm/360 nm Pattern

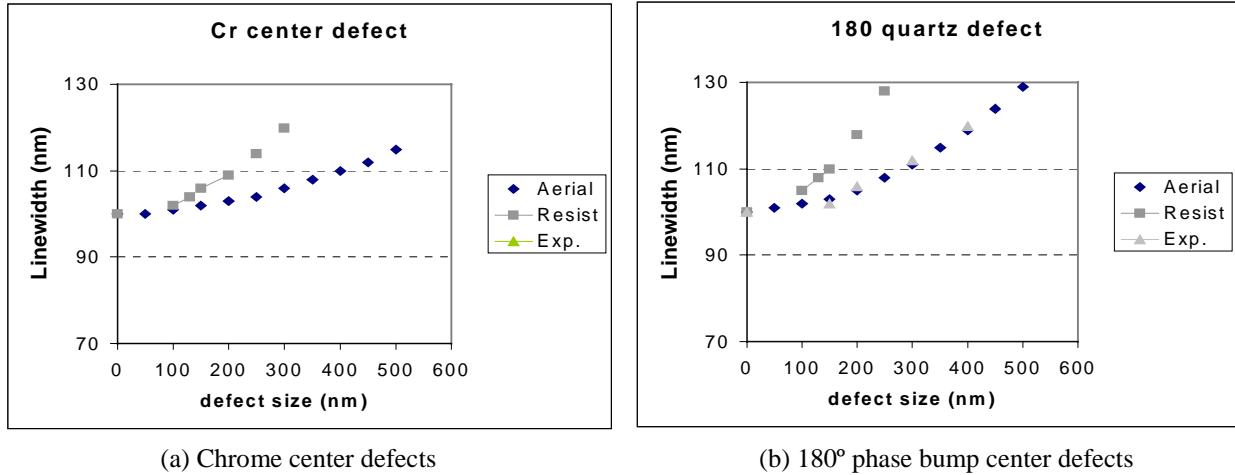


Figure 12 Defect Size vs. Linewidth Comparison Between Aerial Image and Resist Simulation of L/S = 100 nm/400 nm Pattern

Table 2 MNPD Size Comparison Between Aerial Image Simulation and Resist Simulation

	L/S=140 nm/360 nm		L/S=100 nm/400 nm	
	Chrome center	Phase center	Chrome center	Phase center
2D aerial image	350	250	350	250
Resist simulation	220	205	200	150
Experiment	320	265	—	250

From these resist simulations, it was found that traditionally defined MNPD showed around 70% process overlap between defect pattern and no defect pattern, as shown in Figure 13 and Table 3.

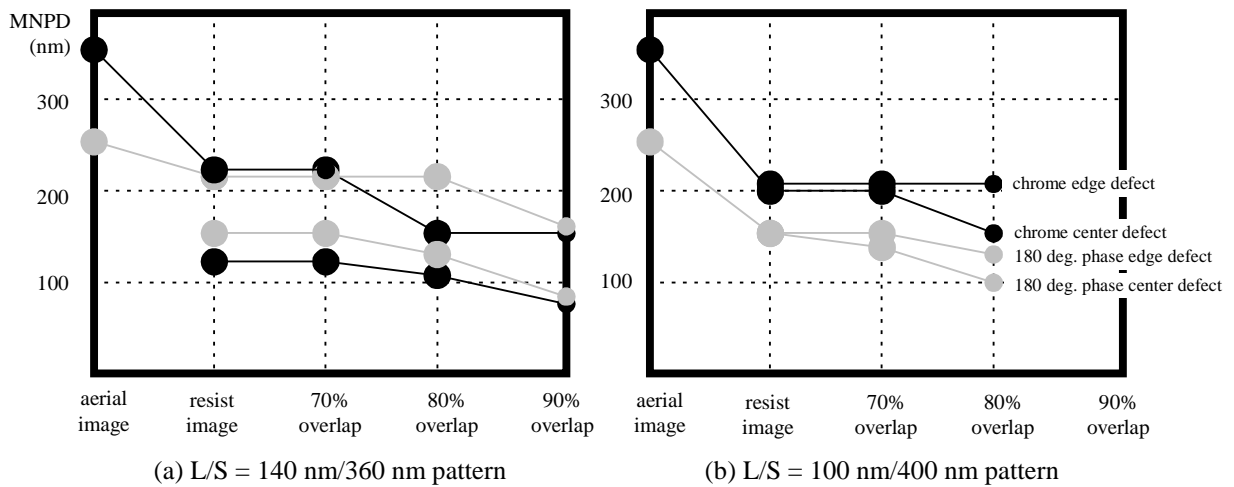


Figure 13 Simulated Result Comparison Between Defocus Only and Expose/Defocus Window

Table 3 MNPD Size Comparison Between Traditionally Defined Case and Window Overlap Cases by Resist Simulation

	L/S=140 nm/360 nm				L/S=100 nm/400 nm			
	Chrome		Phase bump		Chrome		Phase bump	
	Center	edge	Center	Edge	Center	Edge	Center	Edge
Traditional way	220	120	205	150	200	200	150	150
70% overlap	220	120	205	150	200	200	130	150

4.4 3D EMF vs. 2D Aerial Image Simulation for Phase Defect Printability

Three-dimensional EMF simulation was applied for phase bump defects and divot defects to compare with 2D simulation, as shown in Figure 14.

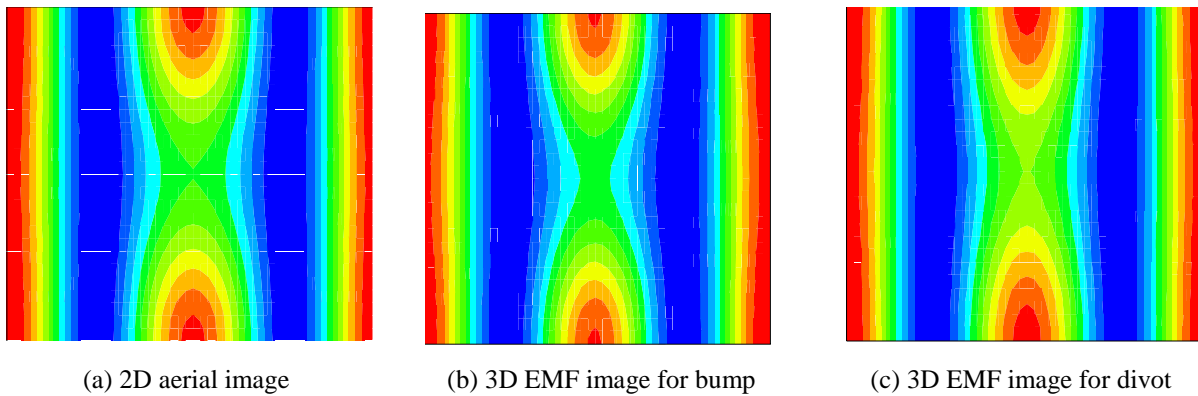


Figure 14 Aerial Image Comparison Between 2D Simulation and 3D EMF Simulation of L/S = 140 nm/360 nm Pattern with 390 nm Phase Defect

It was found that 2D simulation underestimates defect printability for phase bump center defects, while it estimates similar to 3D EMF simulation for phase divot defects of L/S=130 nm/370 nm, as shown in Figure 15.

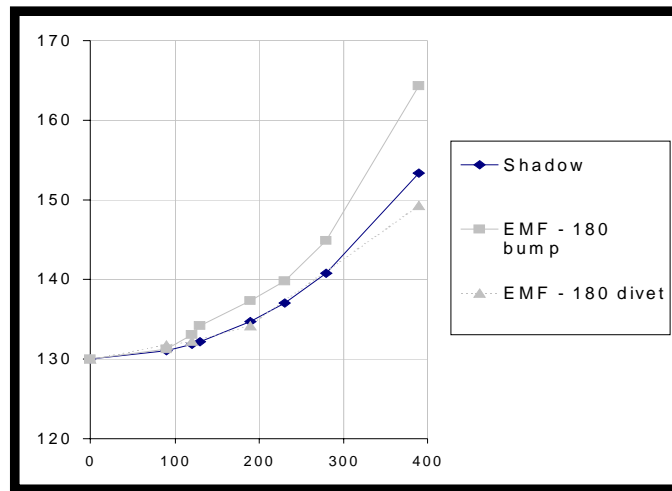


Figure 15 Defect Size vs. Linewidth Simulation Plot Comparison Between 2D Aerial Image Simulation and 3D EMF Simulation of L/S = 130 nm/370 nm Pattern

When a denser pattern of L/S=100 nm/200 nm is considered, the printability difference between 2D simulation and 3D EMF simulation increases as shown in Figure 16.

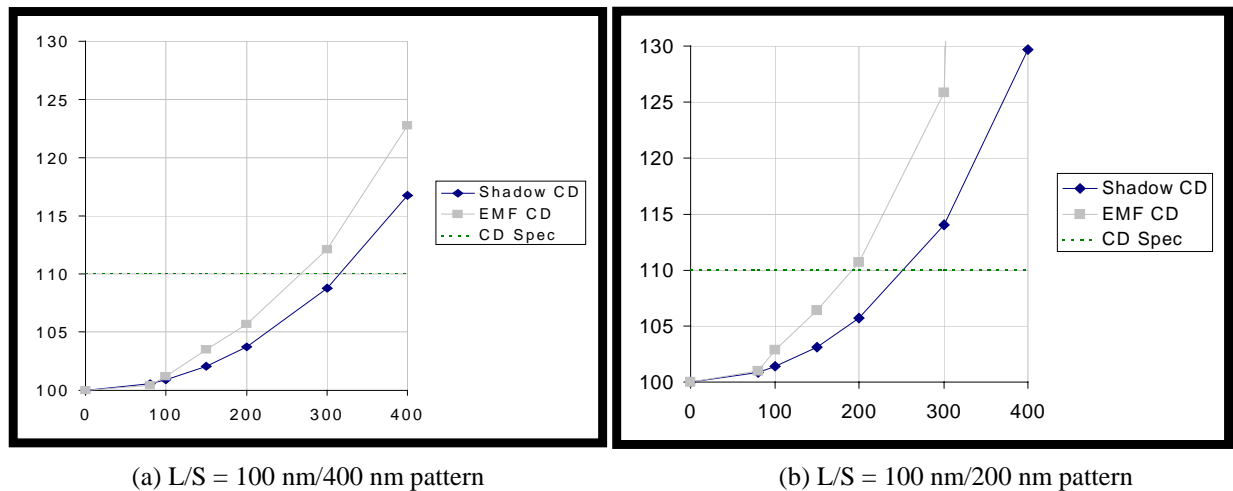


Figure 16 Defect Size vs. Linewidth Simulation Plot Comparison Between 2D Aerial Image Simulation and 3D EMF Simulation of 1:4 Duty Ratio Pattern and 1:2 Duty Ratio Pattern

A 2D simulation showed that phase bump edge defects are more printable than phase center defects, but 3D EMF simulation did not show a difference between center and edge defects at pattern of L/S=140 nm/360 nm, as shown in Figure 17 and Table 4.

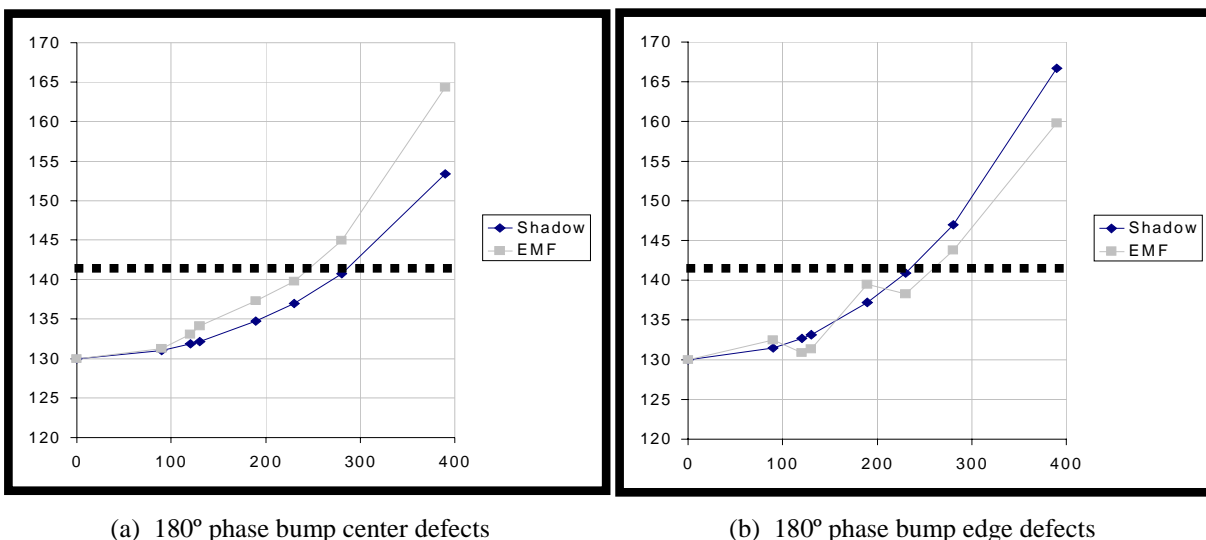


Figure 17 Defect Size vs. Linewidth Simulation Plot comparison Between 2D Aerial Image Simulation (Shadow) and 3D EMF Simulation of L/S = 30 nm/370 nm Pattern

Table 4 MNPD Size Comparison Between 2D Aerial Image and 3D EMF Simulation

	L/S=140 nm/360 nm				L/S=100 nm/400 nm	
	Phase bump		Phase divot		Phase bump	
	Center	Edge	Center	Edge	Center	Edge
2D aerial image	280	230	280	—	300	—
3D EMF simulation	230	230	280	—	200	—

4.5 Defect Printability Prediction for Denser Pattern of L/S=130 nm/130 nm

Even though experimenters found out that aerial image simulation could predict the defect printability for the pattern of L/S=140 nm/360 nm, 100 nm/400 nm, they are not sure if it works for dense pattern, such as duty ratio 1:1. With the limitations of the mask making process, it is difficult to make programmed defect mask having small defects on 1:1 dense pattern. Therefore, 2D aerial image and resist simulation was applied to see MNPD at denser pattern of L/S = 130 nm/130 nm in this section. Aerial image simulation still predicted big MNPD, 350 nm for chrome defect and 250 nm for phase defect, at 1:1 dense pattern; in this, resist simulation predicted MNPD smaller than 100nm, as shown in Figure 18 and Table 5. Aerial image simulation for defect printability of 1:1 dense pattern does not make sense, based on the simulation and the experimental results from the pattern of L/S=140 nm/360 nm and 100 nm/400 nm. One can predict conservatively that defects smaller than 60 nm will not be printed on this pattern, but exact numbers of MNPD size should be revisited with more analysis on 3D EMF simulation, using actual defect shapes and sizes.

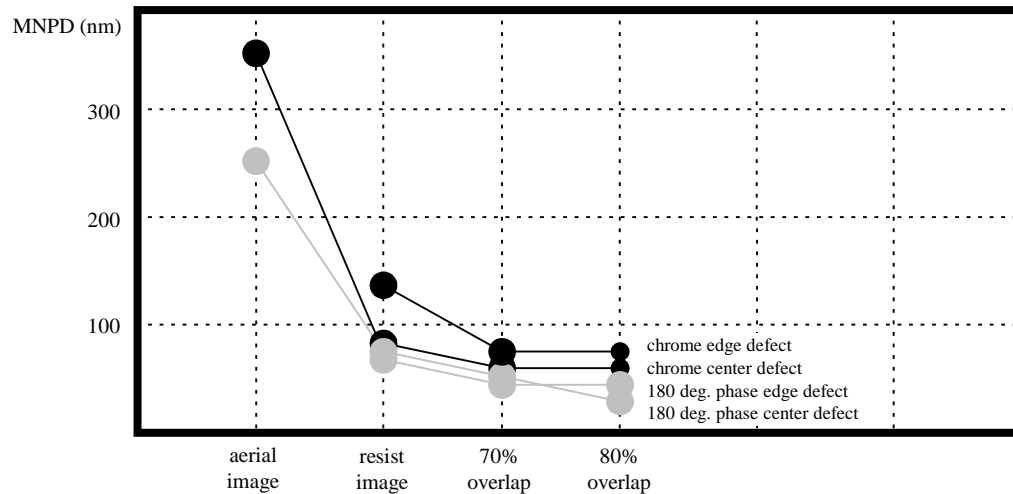


Figure 18 Defect Size vs. Linewidth Simulation Plot Comparison Between Aerial Image and Resist Simulation of L/S = 130 nm/130 nm

Table 5 Simulated MNPD Size for 1:1 Dense Pattern of L/S=130 nm/130 nm

	Chrome		Phase bump	
	Center	Edge	Phase	Edge
2D aerial image	350	—	250	—
Resist simulation	80	130	80	80
70% overlap	60	80	60	60

4.6 Phase Bump Defect Repair

In this section, experimenters tested the mechanical repair tool for quartz bump defect removal, which is being developed by RAVE. Defect pattern was L/S=140 nm/360 nm and repaired defect sizes were 250 nm, 400 nm, and 500 nm for center defects and edge defects. The defect pattern was inspected using AFM, 248 nm AIMS, CD SEM and wafer pattern before and after repair. As a result, phase bump center defects were repaired well enough not to print on the wafer, but edge defects did not work well, as shown in Figure 19. When process windows of defect patterns was examined, it was found that they were fully recovered after repair for center bump defects, as shown in Figure 20 but not for edge bump defects as shown in Figure 21.

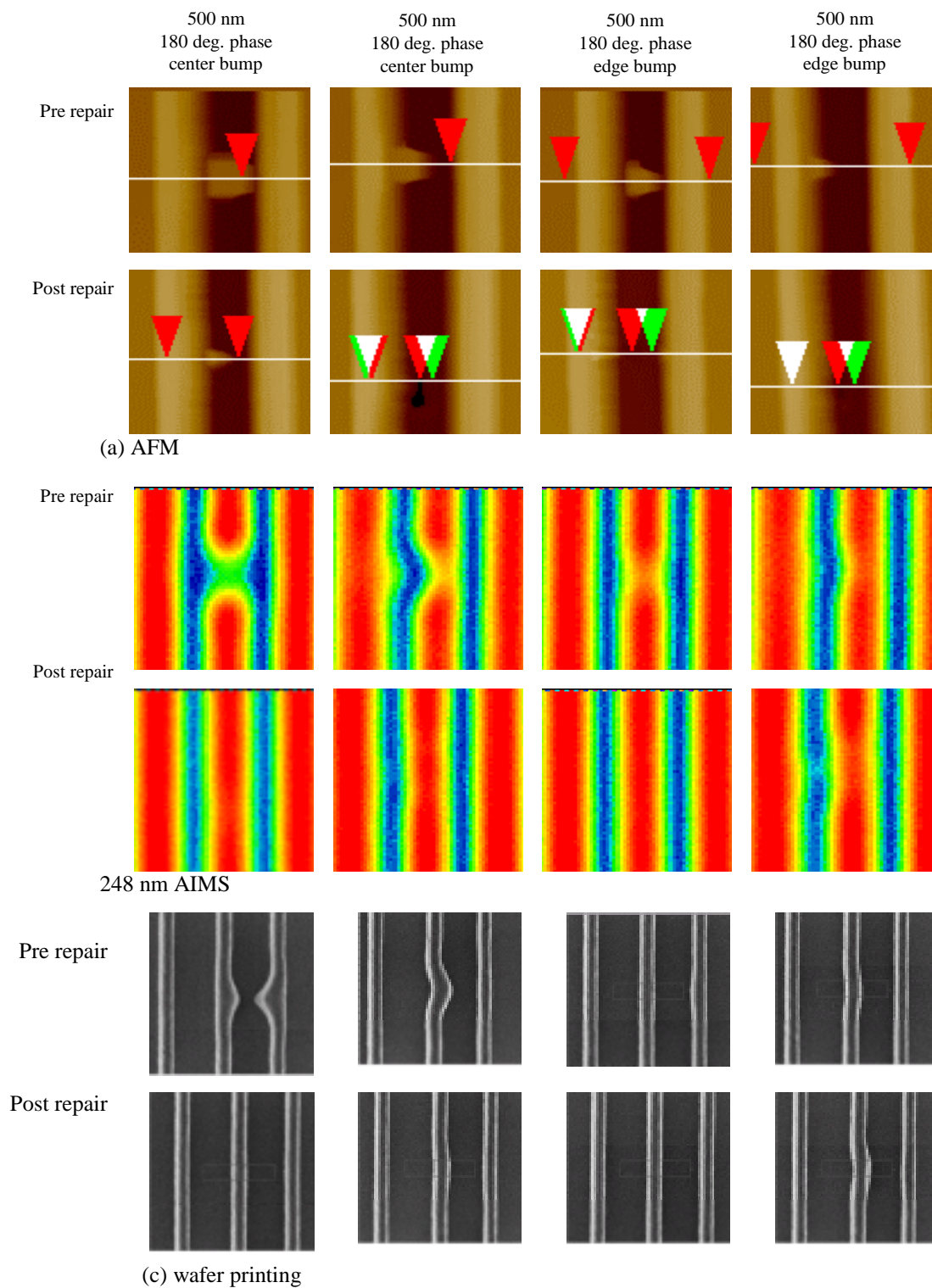


Figure 19 Phase Bump Defect Pattern Images Before and After Repair by Mechanical Removal Tool

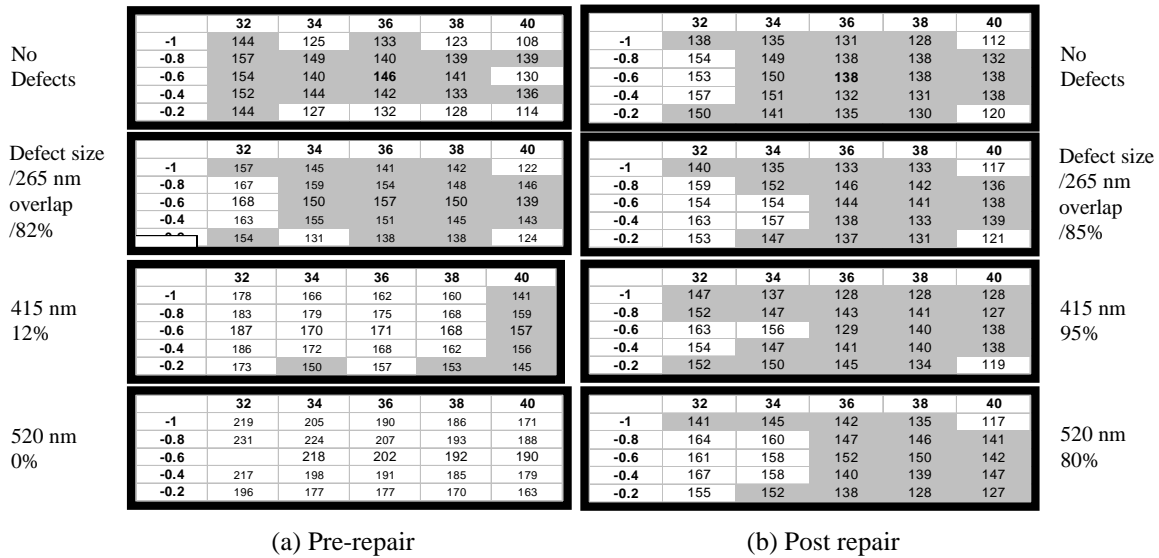


Figure 20 Expose/Defocus Windows of Phase Bump Center Defect Pattern of L/S = 140 nm/360 nm Before and After Repair by Mechanical Removal Tool

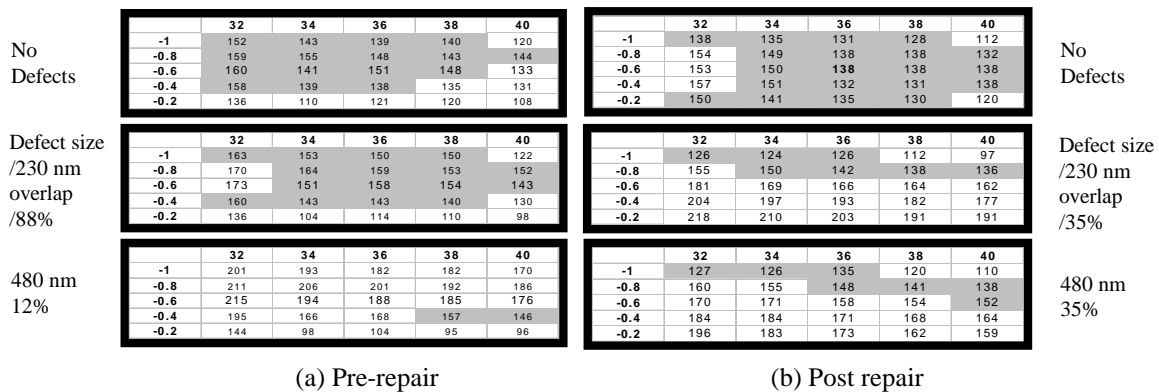


Figure 21 Expose/Defocus Windows of Phase Bump Edge Defect Pattern of L/S = 140 nm/360 nm Before and After Repair by Mechanical Removal Tool

5 CONCLUSION AND FUTURE WORKS

Conclusions from this study are as follows:

- Traditionally defined MNP sizes provided a 70~80% process window overlap between defect pattern and no defect pattern of L/S=140 nm/360 nm and 100 nm/400 nm.
- Two-dimensional aerial imaging showed good agreement with experimental results, while resist process simulation overestimated it.
- Three-dimensional EMF simulation showed that 2D aerial image simulation underestimates defect printability for phase bump center defects, but estimates similarly for phase divot defects.
- Conservative prediction of MNP sizes for chrome defects and phase defects are ~60 nm for L/S=130 nm/130 nm.

- Phase bump defects could be removed well enough not to print on the wafer by mechanical repair tool for center defects.

Future study will include 60° and 120° phase defects for defect printability. Wafer printing testing will be done for phase divot defect patterns to verify 3D EMF simulation.

6 REFERENCES

- [1] T. Yasuzato, S. Ishida, and H. Tanabe “Pattern Dependence of Mask Topography Effect in Alternating Phase-Shifting Masks,” *SPIE* Vol. 3748, pp. 363–370, 1999.
- [2] S. Peng “Through-Focus Image Balancing of Alternating Phase Shifting Masks,” *SPIE* Vol.3873, pp. 328–336, 1999.
- [3] L. Liebmann, S. Mansfield, A. Wong, J Smolinski, S. Peng, K. Kimmel, M. Rudzinski, J. Wiley, and L. Zurbrick “High Resolution Ultraviolet Defect Inspection of DAP Reticles Darkfield Alternate Phase,” *SPIE* Vol. 3873, pp. 148–161, 1999.
- [4] S. Nagashige, K. Hayashi, S. Akima, H. Takahashi, K. Chiba, Y. Yamada, and Y. Matsuzawa “Detection and Repair of Multiphase defects on Alternating Phase-Shift Masks for DUV Lithography,” *SPIE* Vol. 3873, pp. 127–137, 1999.

**International SEMATECH Technology Transfer
2706 Montopolis Drive
Austin, TX 78741**

**<http://www.sematech.org>
e-mail: info@sematech.org**